*Int. J. Electrochem. Sci.*, 16 **(2021)** Article Number: 211122, doi: 10.20964/2021.11.02

International Journal of
ELECTROCHEMICAL
SCIENCE
www.electrochemsci.org

# Effect of surface roughness on the characteristics of passive film formed on 5083 Al alloy in pH 8.4 Borate Buffer Solution

*Junping Chen*[1], *Yanhui Ma*[1],*Jianfen Yin*[1], *Te Hu*[2], *Qiongyu Zhou*[2,*]

[1] North China Electric Power Institute Co.,Ltd, Beijing 100045, China
[2] School of Materials Science and Energy Engineering, Foshan University, Foshan 528000, China
[*]E-mail: mayanhui1985@163.com; zhouzhouqiongyuxf@126.com

*Received:* 19 July 2021 / *Accepted:* 27 August 2021 / *Published:* 10 October 2021

In this paper, the effect of surface roughness on the characteristics of passive film formed 5083 Al alloy was investigated, by using potentiodynamic polarization curve, electrochemical impedance spectroscopy (EIS), Mott–Schottky analysis and point defect model (PDM). It was found that the 5083 Al alloy shows satisfactory passivation performance in the borate buffer solution. The formed passive films exhibit p-type semiconductor characteristic. The smaller surface roughness can promote passive film to form less carrier density and smaller diffusion coefficient, which improved the quality of passive film and enhance its corrosion resistance.

**Keywords:** 5083 Al alloy, Surface roughness, Passive, Corrosion resistance, Point defect model

## 1. INTRODUCTION

Aluminum alloy has been widely used in electric power fields marine, and transportation industries, due to its low density, good electrical conductivity, high strength and excellent corrosion resistance [1-4]. Generally, compact oxide layers would be formed on surface of aluminum alloy in many environments [5, 6]. Due to the passive nature, aluminum alloy shows exceptional general corrosion resistance when exposed to air, acid, alkaline or some chloride-containing solution [7-9]. However, localized corrosion (intergranular corrosion, exfoliation corrosion, stress corrosion, pitting, etc.), which is related to the heat surface abrasion, treatment processing, workpiece structure, and service environment, is unavoidable and closely affected by the quality of formed passive film. Therefore, research on the passivating of aluminum alloy has drawn lots of attention [10-12].

Point defect model (PDM), which is proposed by D. D. Macdonald, has been demonstrated to be an effective approach to describe the characteristic semiconductor properties of the passive film [13-15].

Nowadays, PDM is mainly employed to study the passive film formed on the surface of stainless steels, iron, nickel-base alloys and cobalt-base alloys [16-20]. The research on the semi-conductive properties of passive film on the aluminum alloy is quite rare [11].

5083 aluminum alloy is a typical shell material of the Gas Insulated Switchgear (GIS) [21]. The corrosion of GIS shell would decrease stability of electrical power system and cause a lot of pollution by reason of leakage of $SF_6$ gas [22]. Especially, 5083 aluminum alloy is susceptible to localized corrosion, because of its complex precipitation on the grain boundaries [23].In view of the surface states is a critical factor for maintaining the stability of protective passive film, the effect of surface roughness on the characteristics of passive film formed 5083 Al alloy is investigate by Mott-Schottky analysis and PDM in this paper.

## 2. EXPERIMENTAL

The 5083 aluminum alloy samples (11 mm × 11 mm × 2 mm) studied in this work were drawn from the Commercial GIS shell (State Grid Corporation of China) by electrical discharge machining. The chemical composition was detected by inductively coupled plasma atomic emission spectrometer (ICP-AES, Optima-7000DV, Thermofisher) and the results is listed in Table 1. To obtain different surface roughness, the samples were unidirectionally abraded in ethyl alcohol with SiC abrasive paper to 5 grades (100-grit, 800-grit, 2000-grit and 5000-grit), respectively. Accordingly, the polished samples are denoted as S100, S800, S2000 and S5000. The surface roughness were tested by surface texture measuring instrument (Mitutoyo, SJ-310). Then, all samples were cleaned in acetone and deionized water followed by epoxy encapsulation to confirm that the exposed area is 10 mm × 10 mm.

The electrochemical tests were conducted on a PARSTAT VersaSTAT 3F workstation with a classical three-electrode electrochemical cell, which contains Pt sheet (20 mm×20 mm) as the counter electrode, saturated-calomel electrode (SCE) as reference electrode and 5083 aluminum alloy samples with different surface roughness as working electrode. The test solution was borate buffer solution containing 0.15 M $B(OH)_3$ and 0.075 M $Na_2BO_4{\cdot}10H_2O$ (pH=8.4±0.1, open to air, 25 ℃), which was prepared by analytical grade chemicals and deionized water. The potentiodynamic polarization measurements were using a scan rate of 10 mV $min^{-1}$ starting at -0.05 V vs. OCP and ended at the potentials when current density reached to $10^{-3}$ A $cm^{-2}$. In order to form stable passive film, the potentiostatic anodic polarization experiments were performed at the potentials within the passive region (specifically, -1.0 V, -0.5 V, -0.0 V and 0.5 V) for 30 min. Prior to anodic polarization, all samples should be cathodically polarized at $-1.5$ $V_{SCE}$ for 8 min to remove the naturally formed oxide films before anodic polarization. Then, electrochemical impedance spectroscopy (EIS) and Mott–Schottky plots were tested. The EIS measurements were carried out at the open circuit potential (OCP) using a 10 mV AC stimulus signal in the frequency range from $10^5$ Hz to $10^{-2}$ Hz. Mott–Schottky plots were tested in the potential range of -0.4~0.8 V, with scan rate of 0.05 V $s^{-1}$, at the applied frequency of $10^3$ Hz.

**Table 1.** Chemical composition of 5083 aluminum alloy studied in this paper (wt.%).

| Mg | Mn | Fe | Cr | Si | Al |
|---|---|---|---|---|---|
| 5.54 | 0.46 | 0.26 | 0.12 | 0.16 | Bal. |

## 3. RESULTS AND DISCUSSION

### *3.1. Surface roughness*

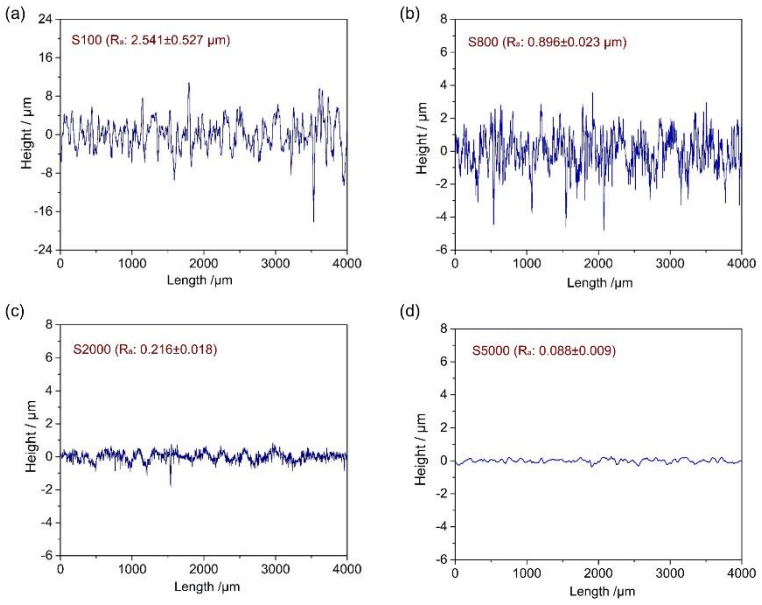


**Figure 1**. The surface profiles of abraded 5083 aluminum alloy samples

The surface profiles perpendicular to the abrasion direction of abraded 5083 aluminum alloy samples are displayed in Fig. 1. It is clear that the average roughness parameters ($R_a$) of S100, S800, S2000, S5000 are 2.541 ± 0.527 μm, 0.896 ± 0.023 μm, 0.216 ± 0.018 μm and 0.088 ± 0.009 μm, respectively. Obviously, $R_a$ values show the tendency that gradually decrease with the increase of grit number.

### *3.2 Potentiodynamic polarization tests*

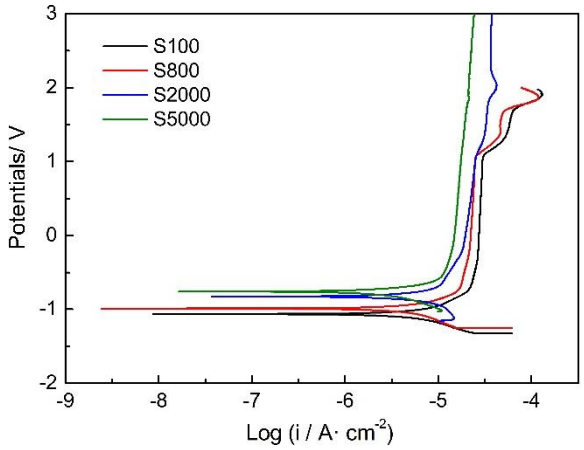


**Figure 2.** The potentiodynamic polarization curves of the abraded 5083 aluminum alloy samples in borate buffer solution.

**Table 2.** The electrochemical parameters extracted from the potentiodynamic polarization curves in Figs. 2.

| Samples | $E_{corr}$ (V) | $i_{corr}$ ($A \cdot cm^{-2}$) | $i_{pass}$ ($A \cdot cm^{-2}$) |
|---|---|---|---|
| S100 | -1.05 | $8.51\times10^{-6}$ | $2.24\times10^{-5}$-$4.01\times10^{-5}$ |
| S800 | -0.98 | $4.63\times10^{-6}$ | $2.00\times10^{-5}$-$2.45\times10^{-5}$ |
| S2000 | -0.82 | $5.75\times10^{-6}$ | $1.34\times10^{-5}$-$3.54\times10^{-5}$ |
| S5000 | -0.75 | $1.15\times10^{-6}$ | $6.31\times10^{-6}$-$2.29\times10^{-5}$ |

Fig. 2.shows the potentiodynamic polarization curves of abraded 5083 aluminum alloy samples in borate buffer solution. It can be observed that there exists typical passivation behavior for the 5083 aluminum alloy, conforming that the protective passive film would be formed on the surface. The corresponding corrosion electrochemical parameters extracted from the potentiodynamic polarization curves are listed in Table 2. As shown, both the corrosion current density ($i_{corr}$) and passive current density ($i_{pass}$) decrease with the decrease of surface roughness (the increase of grit number). The results indicate that the corrosion resistance increases in the order of that S5000> S2000> S800> S100. This phenomenon would can be attributed to the fact that surface roughness influence pitting corrosion by altering the openness of surface grooves and the true surface area. This result is similar to the 2297 Al-Li alloy, which shows less active and shows lower pitting susceptibility for the smoother surface [12]. Considering that the quality of the passive film is a crucial factor for the performance of its corrosion resistance, the basic characteristics of semiconductor passive films are further investigated in this paper, of which the passive films are formed in borate buffer solution by potentiostatic anodic polarization. It should be noted that the operational anode potential must be in the passive region.

### *3.3 EIS study*

Fig. 3 shows the results of EIS tests in the form of Nyquist plots. As shown, all the Nyquist plots display the features of an unfinished semi-circle, which suggests the similar kinetics [24]. No diffusive impedance can be observed in the Nyquist plots, indicating that the corrosion of 5083 aluminum alloy is under activation control rather than under diffusion control [25, 26]. For the same sample, the diameter of the semicircle increase with the increase of applied potential, being similar to that the passive film formed on the surface of copper at higher potential would own an increase corrosion resistance [27].

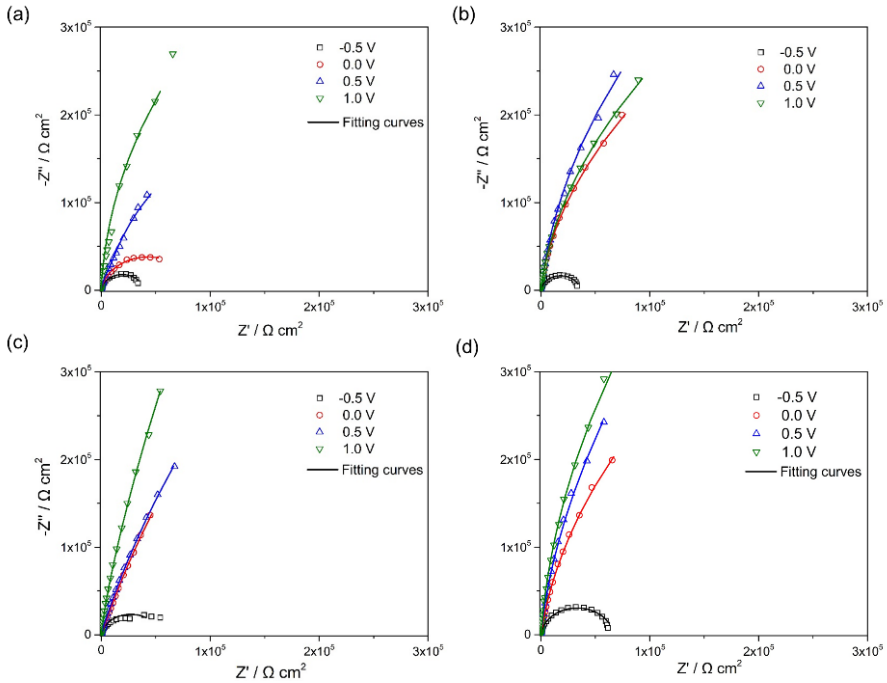


**Figure 3.** The Nyquist plots and fitting results (solid lines) of the passive films formed on the abraded 5083 aluminum alloy samples after potentiostatic anodic polarization at different applied potential in borate buffer solution. (a: S100; b: S800; c: S2000; d:S5000)

To further understand the electrochemical process of the electrode interface, a typical electrical equivalent circuit (EEC) in Fig.4 has been used to fit the experimental Nyquist data and the fitting results displayed Fig. 3 as the colored solid lines [28]. In the EEC, $R_s$ is the solution resistance. CPE (constant phase element,) is used to describe the feature of origin electrode surface capacitance and $R_1$ represents the corresponding resistance. C and $R_2$ is the capacitance and charge-transfer of the protective passive film. The good fitting quality which can be observed in Fig. 3 suggests the appropriateness of the used EEC [29]. The values of C are displayed in Fig.5a. According to the PDM, the thickness of steady-state film ($L_{ss}$) is associated with C, vacuum permittivity ($\varepsilon_0$, $8.854\times10^{-12}$ F·m$^{-1}$) and the dielectric constant of the passive films ($\varepsilon$, 10 for the aluminum alloy), as Eq. (1) [28]:

$$L_{ss} = \frac{\varepsilon\varepsilon_0 \mathrm{A}}{C} \qquad (1)$$

Furthermore, the electric field strength within the passive film ($\varepsilon_L$), which is an important parameter to study the semiconductor characteristics of the passive films, depends on the polarizability ($\alpha$) of the passive film/solution interface and $L_{ss}$. Thereafter, the $\varepsilon_L$ can be calculated according to the mentioned correlative factors as Eq. (2):

$$L_{ss} = \frac{1}{\varepsilon_L}(1-\alpha)E + B \qquad (2)$$

Where $\alpha$ is generally identified to be 0.5 [26]. In Fig. 5b, it is obviously there is a good linear relation between the applied potentials and $L_{SS}$. Therefore, the $\varepsilon_L$ of S100, S800, S2000, S5000 could be ascertained to be $1.89\times10^6$ V/cm, $2.53\times10^6$ V/cm, $3.33\times10^6$ V/cm, $5.05\times10^5$ V/cm, respectively.

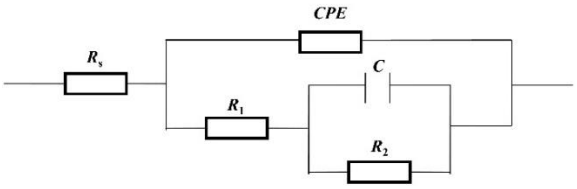


**Figure 4.** The electrical equivalent circuits for fitting the EIS experimental data.

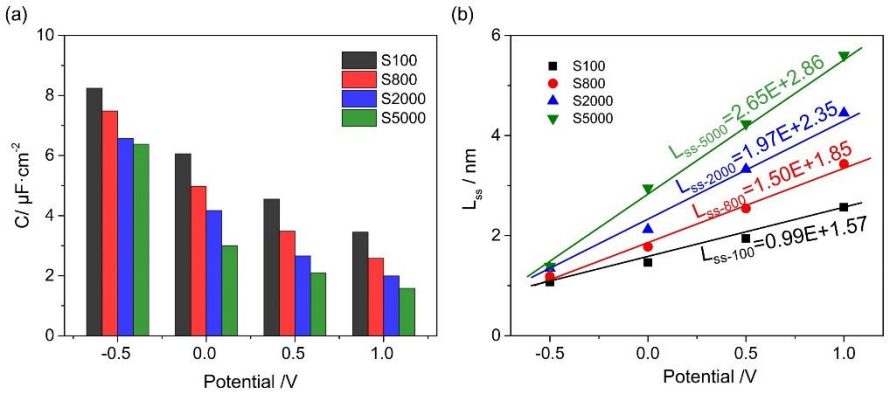


**Figure 5**. (a) The fitted C values for the passive films formed on the abraded 5083 aluminum alloy in borate buffer solution and (b) the $L_{ss}$ at steady-state as a function of the applied potential.

### *3.3. Semiconductor characteristics of the passive films*

Mott–Schottky theory is usually employed to describe the charge distribution state at the interface of semiconductor materials and solution. The space charge capacitance ($C_{sc}$) of semiconductor for a p-type semiconductor contributes to the main of tested capacitance (C) at high frequency ($10^3$ Hz in this paper). Therefore, the $C_{sc}$ can be expressed as Eq. (3) [13, 24]:

$$\frac{1}{C_{SC}^2}=\frac{1}{C^2}=\frac{-2}{\varepsilon\varepsilon_0 eN_A}(E-E_{fb}-\frac{kT}{e}) \quad (3)$$

Where e, $N_A$, k $E_{fb}$ and T are the electron charge ($1.6\times10^{19}$ C), acceptor density, Boltzmann constant ($1.38\times10^{23}$J·K$^{-1}$), band potential and absolute temperature (298.15 K in this paper), respectively.

Fig. 6 shows the Mott–Schottky plots of the passive films formed on the abraded 5083 aluminum alloy. The negative gradient demonstrate the formed passive films show p-type semiconductor characteristic and the dominant defect in the formed passive film are cation vacancies. This is the same as previous studies on the Al alloys, such as the passive film formed on 2099 Al-Li alloy exhibits p-type semiconductor characteristic [11]. The $N_a$ values of passive films formed on the abraded 5083 Al alloy estimated by Eq. (3) are listed in Table 3. As shown, the $N_a$ values decrease with the decrease of the surface roughness. Besides, the $N_a$ value decrease with the increase of applied potential. It can be concluded that the decrease of the surface roughness and nobler applied potential would enhance the corrosion resistance, because of improved passive film quality with lower charge transfer capacity.

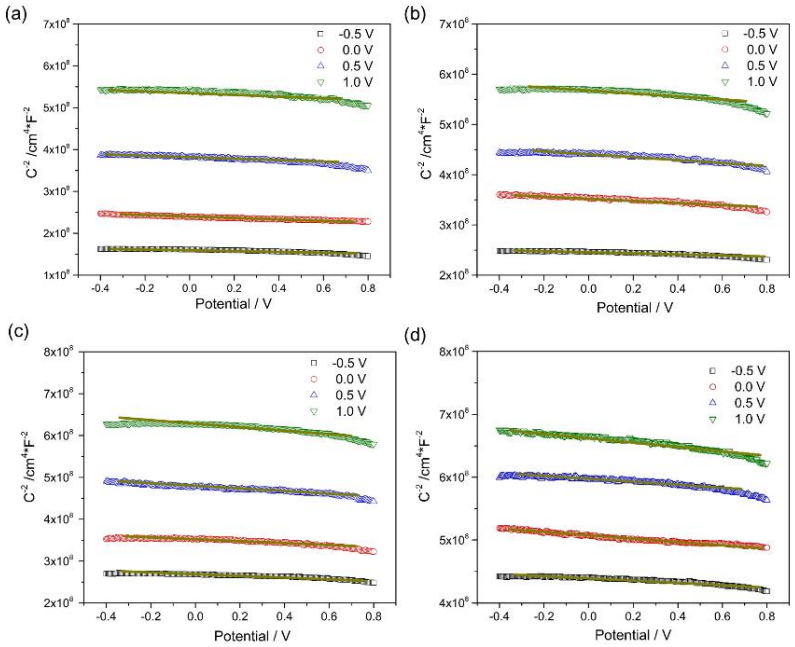


**Figure 6**. Mott-Schottky plots of the passive films formed on the abraded 5083 aluminum alloy in borate buffer solution

**Table 3** $N_a$ values of passive films formed on the abraded 5083 Al alloy ($10^{17}$ $cm^{-3}$)

| Samples | -0.5 V | 0 V | 0.5 V | 1.0 V |
|---|---|---|---|---|
| S100 | 13.2 | 8.24 | 6.52 | 6.14 |
| S800 | 8.98 | 6.21 | 5.24 | 4.56 |
| S2000 | 6.42 | 5.16 | 4.22 | 3.62 |
| S5000 | 4.89 | 4.25 | 3.85 | 3.44 |

Based on PDM, the relationship between $N_A$ value and applied potential E can be defined as Eq. (4) [13, 25]:

$$N_A = \omega_1 \exp(-bE) + \omega_2 \quad (4)$$

Where $\omega_1$, $\omega_2$ and b are three constants which is decided by the nature of formed passive film. Fig. 7 shows the exponential fitting results by using the Eq. (4). The good matched degree shown in Fig. 7a confirms the applicability of PDM. The obtained function are listed in Fig. 7b.

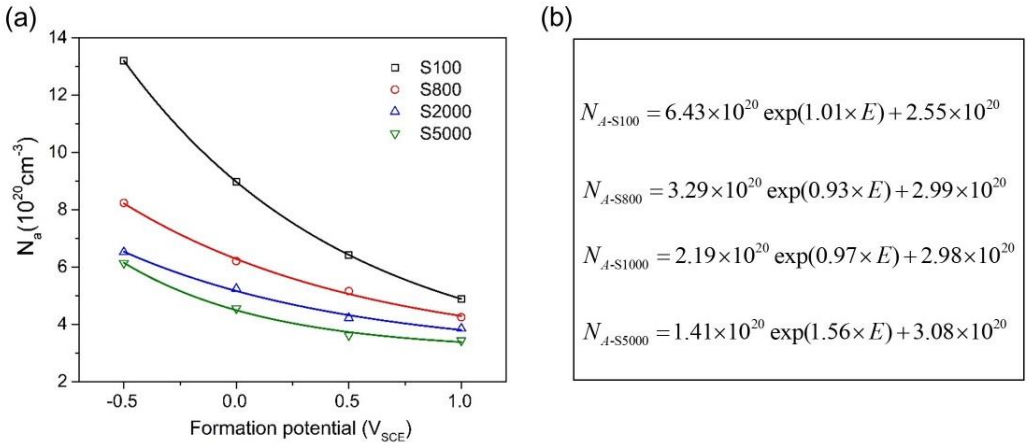


**Figure 7.** (a) The exponential fitting curves and (b) the corresponding functional expression

Afterwards, the diffusion coefficient $D_0$, which is the crucial indicator for describing the kinetics of film growth and the transport properties of the passive film, can be calculated as Eq. (5) [13, 28]:

$$D_0 = \frac{i_{SS}RT}{4eF\varepsilon_L\omega_2} \quad (5)$$

Where $i_{SS}$ is the steady-state passive current density (shown in Fig. 8a). The $\varepsilon_L$ has been obtained from the EIS study. Gas constant R and Faraday constant F are 8.314 J·(mol·K)$^{-1}$ and 96485 C·mol$^{-1}$, respectively. As shown in Fig. 8a, the $i_{SS}$ values during the in borate buffer solution anodic polarization in borate buffer solution are very close to the $i_{pass}$ obtained in the potentiodynamic polarization curves (Table 2). In addition, it can be found that the $i_{SS}$ values are generally decreasing with the increase of surface roughness.

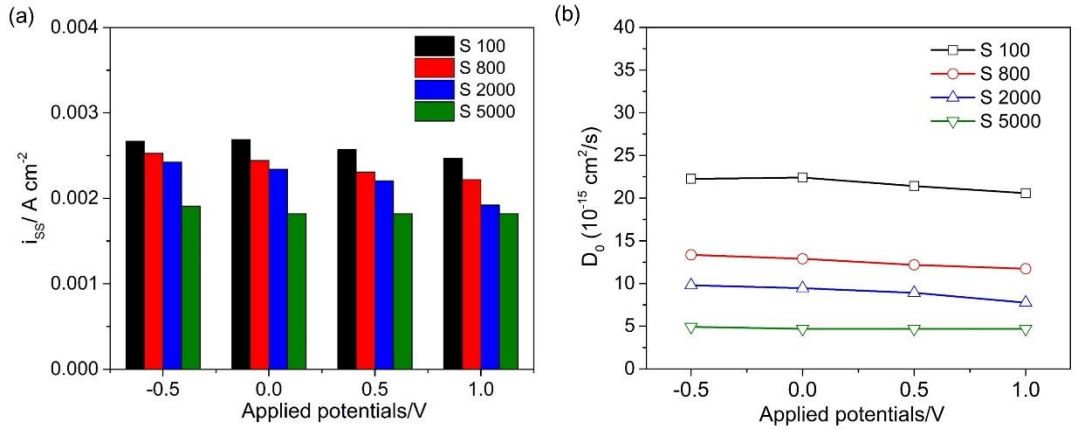


**Figure 8**. (a) $i_{SS}$ for forming the passive films at the steady-state and $D_0$ of the passive films formed on the abraded 5083

Finally, the $D_0$ can be obtained according to PDM and the results are shown in Fig. 8b. The calculated values of $D_0$ of the passive films formed on the abraded 5083 aluminum alloy is in the range of $4.69\times10^{-15}$ cm$^2$ s$^{-1}$–$2.24\times10^{-14}$ cm$^2$ s$^{-1}$. The values of $D_0$ for the same samples are fairly close, while

the values of $D_0$ significantly decrease with the decrease of surface roughness, resulting it kinetic deceleration of the diffusion of corrosive ion in cation vacancy. In summary, the smaller surface roughness can promote passive film to form less carrier density and smaller diffusion coefficient, which improved the quality of passive film and enhance its corrosion resistance.

## 4. CONCLUSIONS

In this paper, the effect of surface roughness on the characteristics of passive film formed 5083 Al alloy. Conclusions can be drawn as follows:

(1) Passive behavior can be observed for 5083 Al alloy in the borate buffer solution. The formed passive films show p-type semiconductor characteristic.

(2) Decrease of surface roughness can decrease the corrosion current density ($i_{corr}$) and the passive current density ($i_{pass}$).

(3) The $\varepsilon_L$ of passive film formed on S100, S800, S2000, S5000 is ascertained to be $1.89\times10^6$ V/cm, $2.53\times10^6$ V/cm, $3.33\times10^6$ V/cm, $5.05\times10^5$ V/cm, respectively.

(4) The smaller surface roughness would promote passive film to form less carrier density and diffusion coefficient, which improved the quality of passive film and enhance its corrosion resistance.

ACKNOWLEDGEMENTS
This work is financially supported by the Key Scientific and Technological Project of Foshan City (1920001000409) and National Natural Science Foundation of China (Grant No. 51764017).

## References

1. I. B. Obot, N. O. Obi-Egbedi and S. A. Umoren, *Int. J. Electrochem. Sci*., 4 (2009) 863-877.
2. J. Wysocka, M. Cieslik, S. Krakowiak and J. Ryl, *Electrochim. Acta,* 289 (2018) 175-192.
3. G. Šekularac and I. Milošev, *Corros. Sci.*, 144 (2018) 54-73.
4. K. Xhanari, M. Finšgar, M. K. Hrnčič, U. Maver, Ž. Knez and B. Seiti, *RSC advances,* 7 (2017) 27299-27330.
5. W. Tian, Z. Li, H. Kang, F. Cheng, F. Chen and G. Pang, *Materials,* 13 (2020) 3236.
6. B. Jegdić, B. Bobić, B. Radojković, J. Kovačina and D. Marunkić, *Trans. Nonferrous Met. Soc. China,* 30 (2020) 1478-1490.
7. S. Bashir, A. Thakur, H. Lgaz, I. M. Chung and A. Kumar, *Surf. Interfaces,* 20 (2020): 100542.
8. M. P. Kumar, P. M. Laxmeesha, S. Ray and C. Srivastava, *Appl. Surf. Sci*., 533 (2020): 147512.
9. P. Kwolek, *RSC Advances*, *10* (2020) 26078-26089.
10. J. Liu, K. Zhao, M. Yu and S. Li, *Corros. Sci., 138* (2018) 75-84.
11. J. Lv, T. Liang., C. Wang and T. Guo, *J. Alloys Compd*., *662* (2016) 143-149.
12. Q. Zhou, Y. Wang, H. Wu, Q. Zhong and J. Jiang, *Surf. Coat. Technol*., 207 (2012) 503-507.
13. D. D. Macdonald, *Electrochim. Acta,* 56 (2011)1761-72.
14. D. Kong, C. Dong, A. Xu, C. He and X. Li, *Corros. Eng. Sci. Techn.,* 52(2017) 188-94
15. A. Xu, C. Dong, X. Wei, F. Mao, X. Li and D. D. Macdonald, *Electrochem. Commun.,* 68 (2016) 62–66.
16. E. Sikora and D. D. Macdonald, *Electrochim. Acta,* 48 (2002) 69-77
17. A. Fattah-Alhosseini, F. Soltani, F. Shirsalimi, B. Ezadi and N. Attarzadeh,. *Corros. Sci., 53*

(2011) 3186-3192.
18. J. Wang, S. Qian, Y. Li, D. D. Macdonald, Y. Jiang and J. Li, *J. Mater. Sci. Technol., 35* (2019) 637-643.
19. C. Man, C. Dong, Z. Cui, K. Xiao, Q. Yu, and X. Li, *Appl. Surf. Sci*., *427* (2018) 763-773.
20. H. Du, Y. Zhang, M. Sheng, W. Liu, Q. Zhou, Y. Wang and Q. Zhou, *Acta Chim. Sin.*, *8* (2011) 881-888.
21. D. W. Zhang, T. L. Shi, S and D. Zhao, *Materials*, *12* (2019) 1784.
22. Y. Qiao, H. Zhang, L. Zhao and Q. Feng, *J. Mater. Eng. Perform.,* 29 (2020) 1-12.
23. W. Wang, W. Chen, X. M. Zhao, D. M. Chen and K. Yang, *Int. J. Hydrogen Energy*, *37* (2012) 18672-18678.
24. H. Luo, Z.Li, A. M. Mingers and D. Raabe,. *Corros. Sci.*, 134 (2018) 131-139.
25. W. Tian, S. Li, X. Chen, J. Liu and M. Yu, *Corros. Sci.*, 107 (2016) 211–224.
26. Y. Deng, R. Ye, G. Xu, J. Yang, Q. Pan, B. Peng, X. Cao, Y. Duan, Y. Wang, L. Lu and Z. Yin, *Corros. Sci.*, 90 (2015) 359-374.
27. Q. Zhou, S. Liu, L. Gan, X. Leng and W. Su., *Mater. Res. Express*, *5* (2018) 116534.
28. X. Leng, Y. Zhang, Q. Zhou, Y. Zhang, Z. Wang, H. Wang and B. Yang,. *Mater. Res. Express*, *5* (2018) 056513.

© 2021 The Authors. Published by ESG (www.electrochemsci.org). This article is an open access article distributed under the terms and conditions of the Creative Commons Attribution license (http://creativecommons.org/licenses/by/4.0/).